Article

Unveiling Falling Urban Trees before and during Typhoon Higos (2020): Empirical Case Study of Potential Structural Failure Using Tilt Sensor

Karena Ka Wai Hui [1], Man Sing Wong [1,2,*], Coco Yin Tung Kwok [1], Hon Li [1], Sawaid Abbas [1,3] and Janet E. Nichol [4]

1   Department of Land Surveying and Geo-Informatics, The Hong Kong Polytechnic University,
     Hong Kong, China; karena.kw.hui@polyu.edu.hk (K.K.W.H.); yt-coco.kwok@connect.polyu.hk (C.Y.T.K.);
     honli@polyu.edu.hk (H.L.); sawaid.abbas@connect.polyu.hk (S.A.)
2   Research Institute for Land and Space, The Hong Kong Polytechnic University, Hong Kong, China
3   Remote Sensing, GIS and Climatic Research Lab (RSGCRL), National Center of GIS and Space Applications,
     University of the Punjab, Lahore 54590, Pakistan
4   Department of Geography, University of Sussex, Brighton BN1 9RH, UK; janet.nichol@connect.polyu.hk
*   Correspondence: lswong@polyu.edu.hk; Tel.: +852-3400-8959

Abstract: Urban trees in a densely populated environment may pose risks to the public's safety in terms of the potential danger of injuries and fatalities, loss of property, impacts on traffic, etc. The biological and mechanical features of urban trees may change over time, thereby affecting the stability of the tree structure. This can be a gradual process but can also be drastic, especially after typhoons or heavy rainstorms. Trees may fall at any time with no discernible signs of failure being exhibited or detected. It is always a challenge in urban tree management to develop a preventive alert system to detect the potential failure of hazardous urban trees and hence be able to have an action plan to handle potential tree tilting or tree collapse. Few studies have considered the comparison of tree morphology to the tilt response relative to uprooting failure in urban cities. New methods involving numerical modeling and sensing technologies provide tools for an effective and deeper understanding of the interaction of root-plate movement and windstorm with the application of the tailor-made sensor. In this study, root-plate tilt variations of 889 trees with sensors installed during Typhoon Higos (2020) are investigated, especially the tilting pattern of the two trees that failed in the event. The correlation of tree response during the typhoon among all trees with tilt measurements was also evaluated. The results from two alarm levels developed in the study, i.e., Increasing Trend Alarm and Sudden Increase Alarm indicated that significant root-plate movement to wind response is species-dependent. These systems could help inform decision making to identify the problematic trees in the early stage. Through the use of smart sensors, the data collected by the alert system provides a very useful analysis of the stability of tree structure and tree health in urban tree management.

Keywords: tree failure; tree risk management; tree stability; smart sensing technology; urban forestry; risk mitigation; arboriculture

1. Introduction

1.1. Ecosystem Services Provided by Amenity Trees

Urban trees are vital to augment livability, from their benefits to ecosystem services, moderation of air temperature [1], sequestration of carbon [2], and cultivating an aesthetically pleasing environment [3]; all of which can enhance life quality and well-being [4]. The loss of trees worldwide, either by deforestation or urban tree felling, is one of the key contributing factors to climate change. Climate action is necessary to achieve a balance of anthropogenic emission and natural absorption to resist global warming. At a city level,

planting trees and increasing canopy cover are a strategy for reducing carbon emissions; therefore, maintaining mature and healthy trees is essential. It is important to model and monitor the response of trees to windstorms, devise effective measures to stabilize trees in the urban landscape, and minimize damage to human life and infrastructures.

1.2. Consequences of Tree Failure in Developed Landscapes

Tree uprooting events can also be dangerous to pedestrians. The physical and biological environments in densely populated cities are not always favorable to trees. In urban tree management, it is fundamental to maintain the good health of the trees. This can be achieved by monitoring and mitigating tree risks to prevent damage and disturbances brought about by tree failure cases in the city. Tree risk management includes the process of identifying hazards and determining the degree of danger these hazards pose to the public [5]. Dangerous trees with untreatable problems need to be removed as soon as possible to safeguard the public [6]. Consequences such as traffic dysfunction, property damage, and injuries may cause death in serious cases [7,8].

The microclimate, root–soil system, and other environmental conditions, such as terrain and topography, are significant factors affecting tree stability [9,10]. For each individual tree, the presence of internal and external defects, the elastic modulus of soil and trunk, trunk and crown geometry, and root architecture all affect the response of load-deflection of tree trunk and root anchorage [11]. Researchers have routinely simulated trees and their failures to understand the response of particular species, including under storm events [12]. Sometimes, these controlled trials are also modeled using wind simulation post-rainstorm to demonstrate the correlation between trees and high wind or strong wind gusts [13,14]. Under future climate regimes, the likelihood of tree failure is predicted to further escalate in tropical and sub-tropical countries, thus increasing the susceptibility of urban trees to more precipitation and intensified wind [14,15].

In Hong Kong, Super Typhoon Mangkhut in 2018 necessitated the issuance of Hurricane Signals and brought damaging winds with maximum sustained wind above 185 km/h near the center and a record-breaking storm surge, with over 60,000 urban trees reported to have fallen in the city [16]. Another remarkable Typhoon was Higos in 2020, with a maximum sustained wind of 130 km/h, which hit Hong Kong, with more than 800 fallen trees reported within 22 h [17]. Consequently, as more tree collapse occurs in cities, human exposure to hazardous tree events is expected to increase [18].

Moreover, urban trees can fall faster than anticipated, and not all trees collapse during windy days or storm events. An incident occurred when a tree suddenly fell inside a park on a peaceful sunny day, killing a woman passerby in Singapore. The tree was diagnosed in a tree risk assessment half a year earlier and rated healthy without any discernible signs of potential tree failure [19]. Tree stability can be affected by different biophysical properties in nature, varying by soil cohesion, soil types, root structures, wood density, and wood strength [20]. Tree management objectives have been set out by governments to maintain healthy trees and mitigate risk [21,22]. However, these still lack efficient tools for continuous monitoring of tree health and for quantifying tree risk based on current advanced technology [23].

Additionally, trees respond to the urban environment in highly dynamic and sophisticated ways, as many factors influence uprooting failure, including tree geometries, species, tree age, mass, elasticity, and wood density, in addition to the extent of decay, all of which can significantly impact wind resistance [24–26]. Thanks to human management, the adaptive capacity of urban trees varies substantially according to the array of environments of streets, parks, and roadsides, and they could exhibit adaptive features very different from natural forests [27–29]. For example, a park tree would have a more extensive root structure and moister soil than that of a drier roadside tree in compact paved soil [30].

Every year prior to the rainy season, tree management officers in Hong Kong are required to complete tree risk assessments in areas with high pedestrian and traffic flow, as well as implement appropriate risk mitigation measures. Tree inspection personnel

perform field inspections to examine and assess various health conditions and the structure of a tree. Sometimes it is necessary to climb up the tree to inspect the hidden parts from different angles. Despite requiring an abundance of manpower and resources to cover all urban trees (more than 1,700,000 trees) in the whole territory of Hong Kong [16], tree inspection involves understanding the perceived risk of each urban tree [31] to ensure early preservation of trees, which can help minimize risk exposure for city dwellers [32,33].

However, urban tree itself exhibits unique characteristics and varying amounts of visible and invisible defects, such as dead wood, weak branch union, decay, cankers, severing roots, and poor architecture [34]. Jackson et al. [35] suggested that poor tree architectures would affect tree motion of both conifer and broadleaf trees. Some trees might have more than one defect and significantly affect tree growth, while urban trees in Hong Kong are commonly planted in confined spaces, and the trunk's base is sometimes covered by concrete materials and poor soil conditions [36]. As time goes by, the structural defects would largely reduce the load-bearing capacity of the tree, thereby being more prone to tree failure and tree may even fall when the applied loads are not very large [37].

1.3. Review of Tree Failures during Windstorms

Understanding tree response in heavy windstorms would help urban foresters to identify and minimize human exposure risk and inform the decision for better storm preparedness and management. Many previous studies have investigated the effect of tree sway on wind loads. Lee et al. [38] measured the branch sway behavior of healthy and defective branches of broadleaf trees using a triaxial accelerometer, showing that the mean sway amplitudes of selected branches were correlated to the wind motion. Göcke et al. [39] examined the wind resistance of urban trees by analyzing the correlation between root-plate inclination and regional wind data to obtain the critical wind speed for urban tree failure. However, tree stability may vary after successive storms [40], and therefore, long-term monitoring to assess tilt variation of urban trees is very important [33,41]. Duryea et al. [42,43] statistically measured the impact of three successive hurricanes on the urban forest, demonstrating that native species with decurrent growth form have greater tolerance to high wind. Pull tests were conducted by James et al. [44,45] to obtain an angle close to critical failure with an experimental threshold angle of about 1°, yet under dynamic wind load, the threshold tilt angles were speculated to be 20% higher than the result obtained from the static pull test, based on the study of Stellier [46], or for example, 1.2° or even more for some species. More importantly, Duryea et al. [43] concluded that no tree is completely windproof, while other factors such as defects, severity of decay, and site conditions may affect the wind resistance of a tree. Fewer studies have considered the tilt variations of large-scale urban trees in response to environmental variables to analyze and predict tree failure. There is therefore a need for a comprehensive tree monitoring system to address the above issues, and to provide continuous monitoring and early identification of trees with potential hazards.

1.4. Objectives

The main goal of the present study is to demonstrate: (1) the root-plate tilts before and during Typhoon Higos of two trees that failed during the typhoon; and (2) a CFD model of wind velocity to determine additional insights into two trees; and (3) investigate the correlation between tree tilt angles during Typhoon Higos and corresponding tree attributes. Further to the pilot study of Abbas et al. [47], this study analyzed the variations in tilting patterns that might potentially help identify the relevant tree failure patterns to screen out the problematic trees in the early stage. This can provide valuable data for the development of future contingency plans under typhoon events to mitigate hazard exposure to humans and property, as well as assist in devising effective tree management strategies (Figure 1).
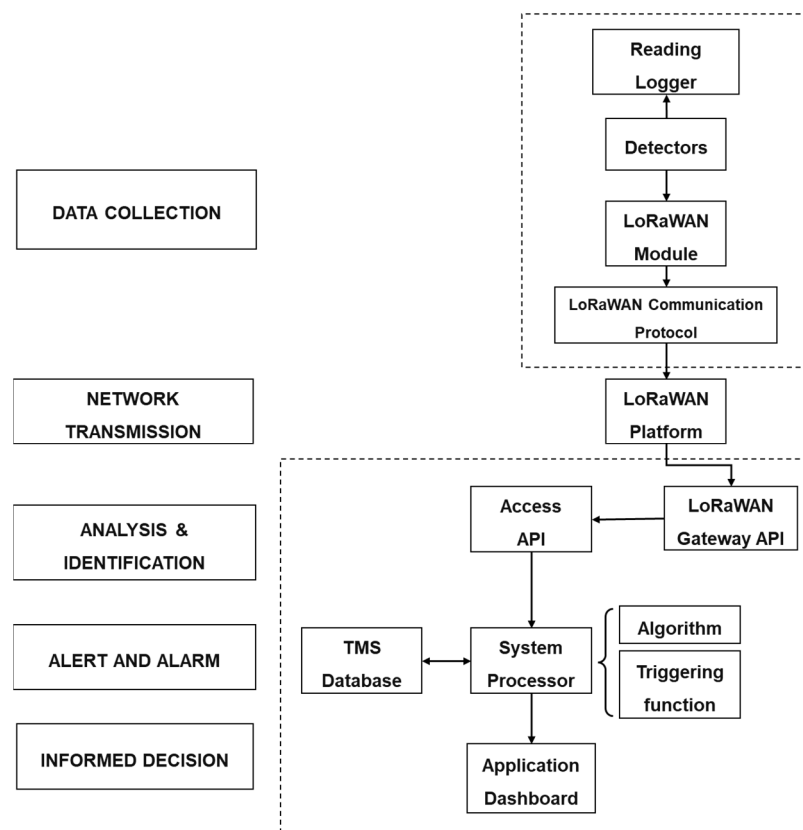
Figure 1. The schematic flow of the study, including data collection, network transmission, analysis and identification, alert and alarm, and informed decision.

2. Methods

2.1. Study Area

Our target area of study is the subtropical city of Hong Kong, located on the south coast of China, with a total land area of 1110 square kilometers. Frequent typhoons occur in the hot and humid summer, alongside occasional thunderstorms and rainshowers. In 2020, the annual mean temperature was 24.4 °C, and the annual total rainfall was 2395.0 mm [48]. According to the statistical figures from the Hong Kong Observatory, 35 tropical cyclones affected Hong Kong between 2015 and 2020 [49].

2.2. Typhoon Higos

The typhoon came close to Hong Kong over 22 h from 18 August 2020 to 19 August 2020, with a maximum centered wind speed of 130 km/h, and was accompanied by precipitation of 119.5 mm. The Kai Tak weather station, the nearest meteorological weather station to the study area, is located at 3 m above sea level (22°18′35″, 114°12′48″). A maximum wind gust of 88 km/h and maximum of 10-min sustained wind speed of 53 km/h during Higos (2020) were recorded. Figure 2 shows the distribution of 889 urban trees with sensors installed. Two trees were found to have been uprooted during Higos (2020) where they are located in between the residential and industrial buildings in the densely built environment, i.e., T_a in Kwun Tong (22°30′26″, 114°01′52″) and T_b in Wong Tai Sin (22°29′52″, 114°02′08″).
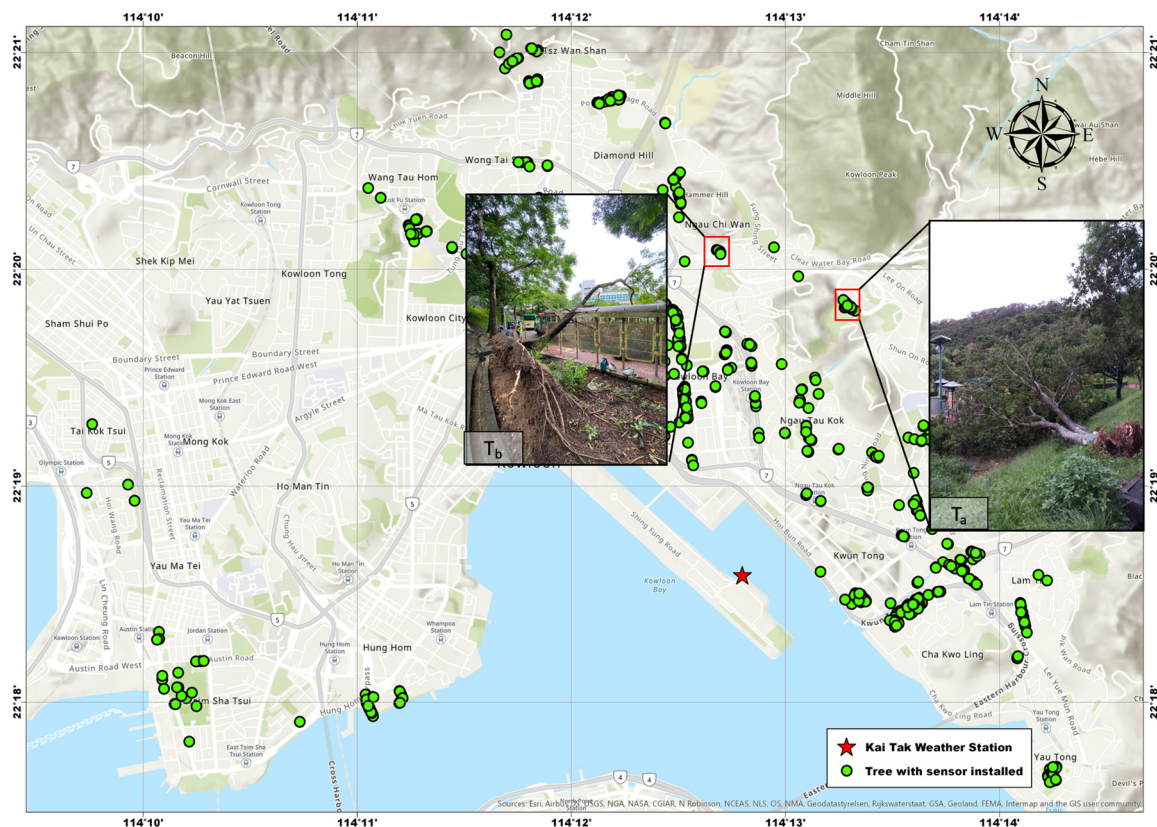
Figure 2. The study area shows two fallen trees, T_a and T_b, located in Kwun Tong and Wong Tai Sin, respectively, and the distribution of 889 trees with sensors installed over urban Hong Kong.

The sensors were installed on 18 local common failure tree species, e.g., *Ficus macro-carpa*, *Delonix regia*, and *Celtis senensis*. A combination of site environments, such as urban parks, street sides, and concrete slopes, were considered as tree selection criteria for the study. Apart from the species and different microclimate environments, the physical properties of trees were also considered as the selection requirement, i.e., the diameter at breast height (DBH) greater than 200 mm; tree height greater or equal to 5 m; and high priority was given to trees along roads and streets with heavy vehicular traffic and pedestrians.

2.3. Tailor-Made Smart Sensors

The tailor-made smart sensor is made up of an accelerometer and gyroscope, which measure the acceleration and direction of root system movement so as to determine the degree of root system displacement against the dynamic wind (Figure 3). A high-sensitivity sensor can measure a very small change in tilt angles in relation to the tree motion response. The accuracy and precision of angle measurements of roll and pitch angles reached 0.1° and 0.01° respectively. The encrypted information, including roll and pitch (in degrees) and air temperature, is transmitted to the cloud server via the low-power wireless communication network, namely the LoRaWAN network, and the data is stored in our local database [47]. The sensor is designed and manufactured to be durable and weather-proof and powered by a longer battery life [50].

Considering that every tree structure is different, the location to install the sensor is important to ensure data consistency. As very few studies have considered sensor measurement for similar purposes, this study has thus developed a protocol to install sensors based on extensive arboriculture experience. The sensor is placed on the lower tree trunk at a height of 0.5 m above the ground and is sometimes installed at the lowest reachable position when the tree is located on inaccessible slopes. This strategy enables higher precision in root-plate measurement under both high wind and natural wind

conditions by reducing the impedance effect from the elastic tree trunk that may potentially add interference to the collected data [27]. The sensor is securely installed on the tree trunk using sterilized stainless-steel screws with lengths not exceeding 5 cm, minimizing the detrimental effects to the living xylem tissues under the tree bark (Figure 3).

Figure 3. Sensors are fixed with the appropriate length of the screw at the position at the lower tree trunk at the height of 0.5 m or the lowest reachable position near the ground.

This is considered the first-ever project in Hong Kong to measure the natural swaying and falling of live trees within urban areas over a long-term duration—i.e., over two years of continuous monitoring. The smart sensor incorporates a logical condition. If additional load or vigorous impact is acting on the sensor leading to tilt variation, for instance, lightning strike, the vibration component equipped in the sensor would be triggered to record data immediately regardless of the preset sampling interval, in order to capture situations caused by unprecedented incidents.

2.4. Sampling Procedure

As typhoon Higos approached, each sensor takes samples every 5 min and transmitted the resultant tilt angles that were calculated from the collected roll and pitch measurements (Figure 4) [47]. By comparing the tilt variation, the tree sway patterns under various circumstances could be interpreted as the magnitude of change in the tilt angles. If a high level of tilt variation or continuous excessive movement is recorded, the tree is identified as unstable or at relatively high risk of failure in high wind. This study will also correlate tilt angle and wind data, investigating the effect of wind load on the affected trees in pre, during, and post-typhoon days. The collated data includes 889 urban trees of different species, coupled with sampling intervals ranging from 5 min to 3 h subject to the weather conditions. Millions of data points are collected, and the sampling interval is changed to 5 min before and during the rainstorm when Higos approached, to maximize data capture for unprecedented changes in tree lean. The sampling interval automatically reverts to 3 h by preset command in the monitoring system when all typhoon signals are canceled. These hybrid modes can save the battery's operational power capacity of at least two consecutive years, thus achieving a greater cost-effective benefit throughout the 3-year study.

All datasets are resampled to 1 h, ensuring continuous tree motion responses being captured. However, electronic sensors are susceptible to temperature drift, due to seasonal temperature variations. To offset the outliers, a temperature compensation algorithm using temperature data is applied to the dataset. The in-situ temperature data is collected from a microsensor, which is one of the components inside the remote-tilt sensor. If X_t denotes the value of the tilt angle in the time series, then the first difference of the tilt angle at 60 days (ΔX) is equal to:

$$\Delta X = X_t - X_{t-60} \tag{1}$$
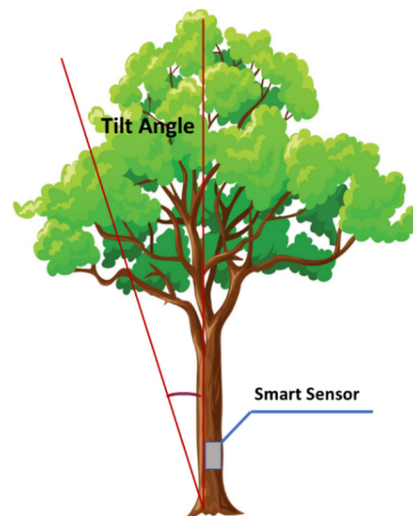
Figure 4. The resultant tilt angle is derived from the roll and pitch measurements along the vertical alignment of the tree trunk.

To compute the Z-score of the ΔX, the rate of change in tilt angle (ΔX) between the percentiles of 10% and 90% is clipped in data pre-processing throughout the entire time-series of the collected sensor data, whereas the Z-score is the threshold that triggers the alarms developed in this study.

In order to screen the data for suspected problematic trees, two alarm systems—the Increasing Trend Alarm and Sudden Increase Alarm— are developed for capturing long-term changes, as well as unexpected drastic changes in tilt angles. For the Increasing Trend Alarm, the resampled time-series datasets are compared by calculating the first difference of tilt angles over 60 days. If the Z-score exceeds the threshold values in 3 standard deviations (SD) and the rate of change of tilt angle (ΔX) > 0.5°, the Increasing Trend Alarm will be triggered.

On the other hand, the Sudden Change Alarm will be triggered by calculating the rate of change of tilt angle over a 1-day interval and analyzing the Z-score of the value difference over the entire time-series data collection period. If the absolute Z-score exceeds the threshold values in 3 SD and the absolute ΔX > 0.25°, the Sudden Change Alarm is triggered.

2.5. Statistical Analysis

Data is analyzed with SPSS for analysis of multi-variances. A boxplot for the change of tilt angles against tree species is generated to show the similarities and differences of tilt response in pre-and post-typhoon. Then, the analysis of covariance (ANCOVA) test is conducted to investigate the overall relationship between tilt angle and the covariates, i.e., DBH, tree height and crown spread, subject to some limitations imposed on the dataset. Where significant, the effect of the analysis of variance (ANOVA) is tested to assess the effect of the categorical variables against tilt angle. Differences in these relations are quantified if the results of the ANCOVA test for differences in variables exceeded the 95% confidence level ($p < 0.05$) [51]. To facilitate comparisons, post hoc tests (HSD) are tested to compare the differences between the means of those significant covariates. This could be used to identify and compare the significance of differences between mean values at $\alpha = 0.05$ [52].

3. Results and Discussion

In this study, two qualitative samples—fallen trees T_a and T_b—showcase two specific scenarios among a diverse distribution of 889 urban trees with sensors installed in Hong Kong. Close monitoring of excessive tilt for Tree T_a—*Celtis sinensis* (Figure 5)—and Tree T_b—*Delonix regia* (Figure 6)—throughout the pre- and during typhoon days revealed sway

behavior and a tree fall pattern. The sensor-captured data of fallen trees from both normal weather days and typhoon weather days are utilized to evaluate patterns of tree sway, thus demonstrating the ability to report tilt variations that can predict tree failure.

3.1. Tilt Variation before and during Typhoon Higos for Fallen Trees

For T_a, *Celtis sinensis*, the DBH was 380 mm and the tree height was 8 m, which was situated at the gully top of Jordan Valley Park (Figure 5a). Before Typhoon Higos (2020), root-plate movement fluctuation of around 0.2° was recorded in the first month of monitoring, followed by a sharp increase of tree movement to 35° under a tropical rainstorm in July 2020—a rainstorm with a maximum wind gust of 86 km/h and an eastward prevailing wind direction (red line, Figure 5b). The weakened stability of T_a is likely due to deformed shear in the tree's root-plate, as the data showed permanent displacement in tilt angle and the tree became stabilized at a relatively high tilt, indicating that the tree is collapsing. Meanwhile, the tilt angle of T_a exceeded the threshold values and triggered the Increasing Trend Alarm. The system alerted the project team of potential collapse. Therefore, tree T_a had confirmed tree lean and was partially uprooted, but no further collapse was seen. According to field observation, root anchorage was partly loosened, and the lateral roots were tightly adhered at the leeward side and detached from the ground at the windward side, with severe cavity decay on the inner trunk flare. To further investigate the extent of the current phenomenon, T_a was identified for "close monitoring" to keep track of its tilt variation to see if the tree could regain its anchoring strength and stabilize itself in the following years, as suggested by Detter et al. [12]. Yet, this situation remained unchanged for a month before Typhoon Higos (2020) approached.

The tilt angle of T_a recorded a second significant increase to 80° (red line, Figure 5c). The Increasing Trend Alarm was triggered at the first sign of tilt variation, which implied that the rate of change in tilt angle in the past 60 days exceeded the pre-set threshold values. Moreover, T_a was permanently displaced upon further confirmation with the azimuth plot. The last data showed that tree T_a was inclined to south-east direction at 155°, indicating the landing position of the fallen tree (Figure 5d). Field inspection confirmed that the tree anchorage failed and reached a critical threshold level after an excessive tilt between 60° and 80°, over a few hours of strong wind gusts.

Another notable case example, tree fall T_b, demonstrates another verification of the tree sensor technique by capturing the critical point of failure of tree T_b resulting from tilt angle surge. Tree T_b—*Delonix regia*—was 11.5 m tall and 370 mm in DBH. It was located at an amenity plot near the public transport terminus in Wong Tai Sin. The root growing space of T_b is compacted at the lower rim of the slope side in a 1-m high planter. There is a high risk of injury to pedestrians and damage to property due to congested surroundings. Tree T_b had no apparent motion before typhoon Higos. During the typhoon, a progressive surge in tilt angle was observed over a few hours of the typhoon, and then the movement came to a halt with permanent displacement (red lines, Figure 6a,b). During Increasing Gale or Storm hoisted warnings, the tilt angle of T_b increased sharply to 40°. The Sudden Increase Alarm was triggered when tilt angles increased. Figure 6c showed that the tree sway trajectory eventually came to a halt 240° at a south-westerly bearing. T_b was speculated to have fallen based on the dataset collected by the sensor, although the final tilt angle was not as high as that of tree T_a. A field survey was conducted after the typhoon and T_b was found to be leaning over the glass cover of the bus terminus facility in the southwest direction and the glass cover was damaged.
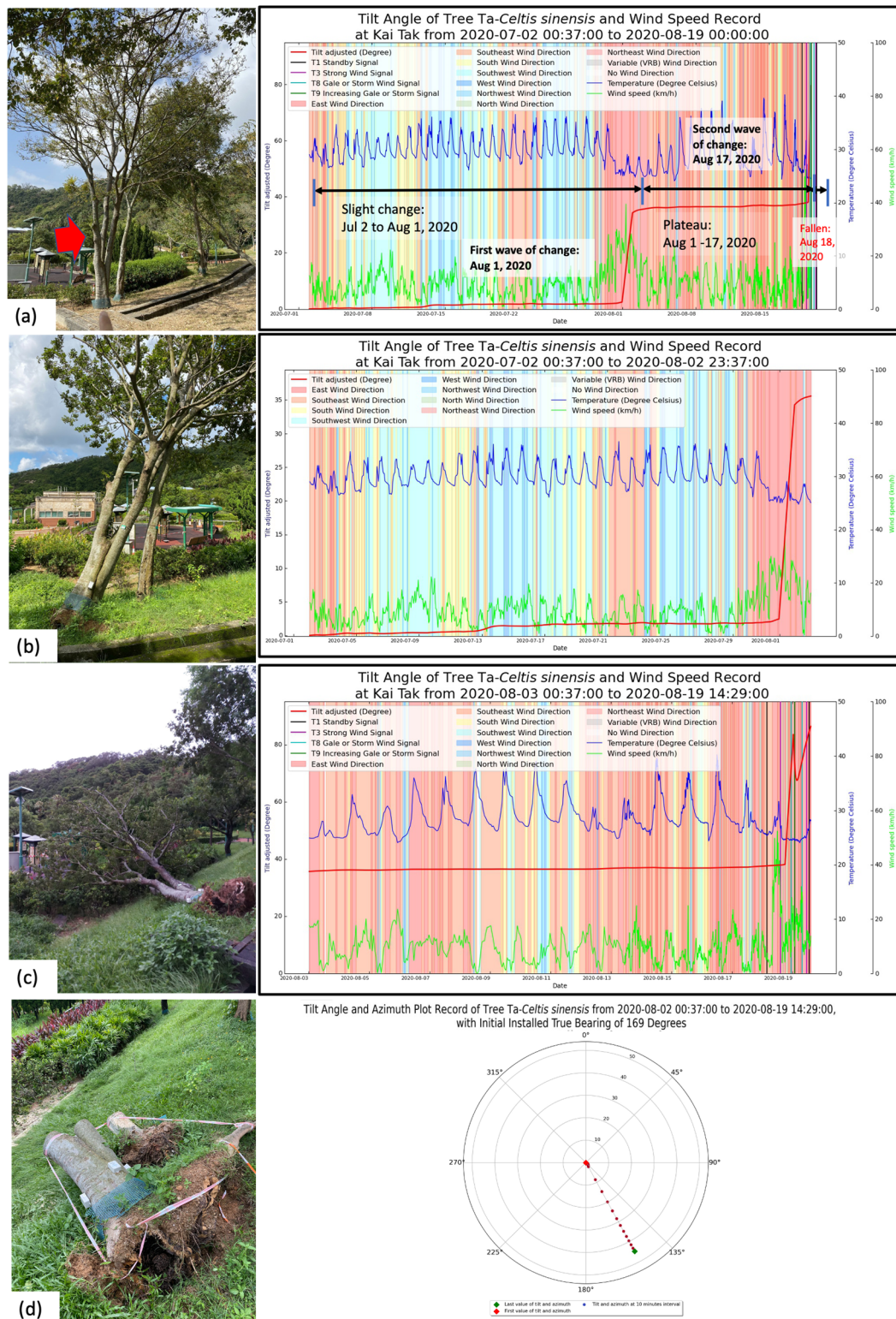
Figure 5. (**a**) The close-up of stable T_a—*Celtis sinensis*. The graph shows the stable fluctuation of 0.2° from 1 July and 1 August 2020, while there was a surge in tilting of T_a from 1 to 18 August 2020 and the Increasing Trend Alarm was triggered; (**b**) after the first wave of tilting, T_a remained with a leaning angle of 35°; (**c**) The fallen T_a in Typhoon Higos. The graph shows T_a was uprooted during Higos with a level of tilt of more than 60° with the Increasing Trend Alarm being triggered; (**d**) The tree was chopped on the day of its collapse. The azimuth plot of T_a fell onto the regions of 135° to 180° with the last data at 155°, representing the tree being landed.
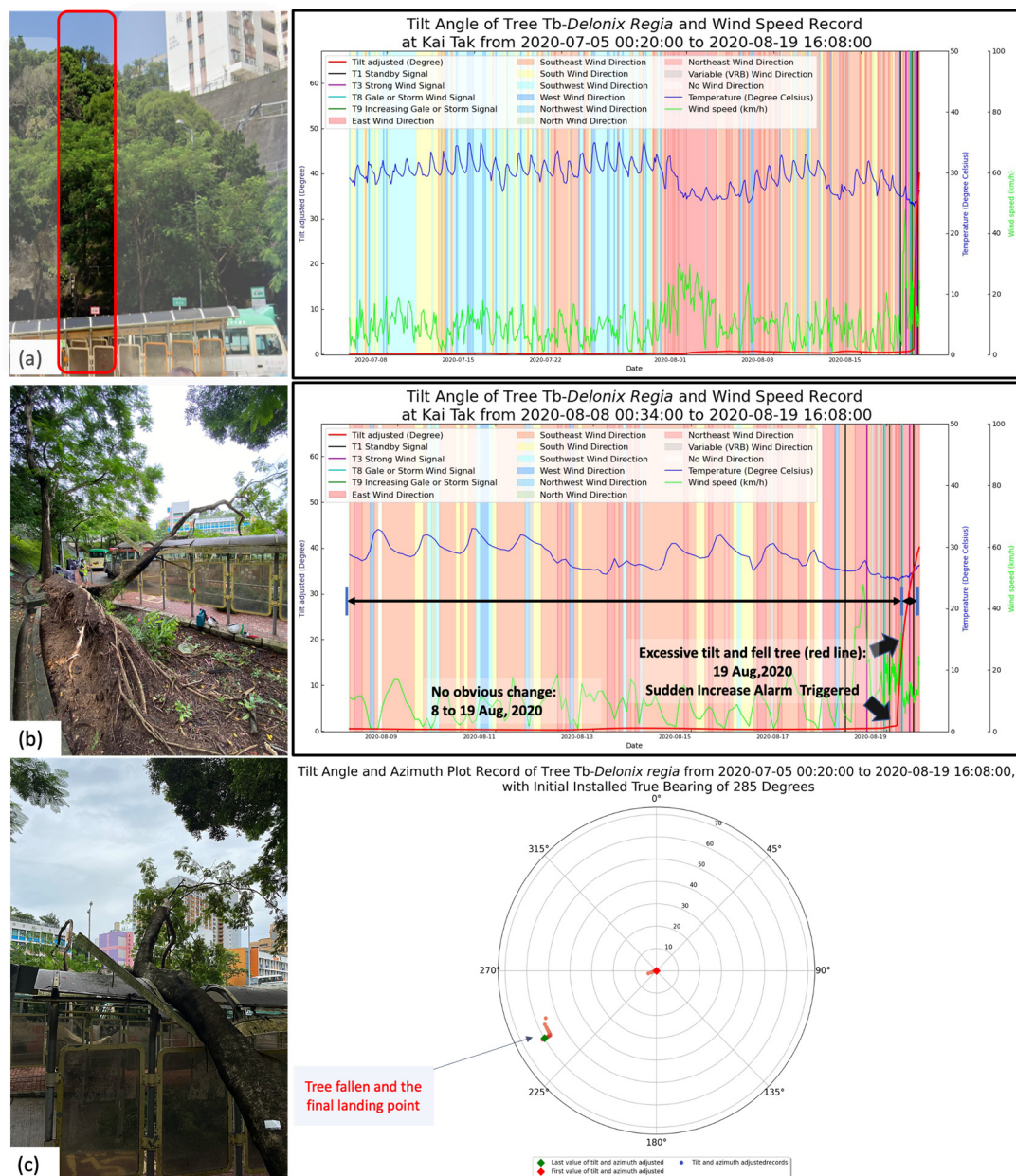
Figure 6. (**a**) The graph shows T$_b$—*Delonix regia*—was recorded stable before Higos (2020); (**b**) The graph shows T$_b$ was uprooted during Higos (2020) on 19 August 2020 with the Sudden Increase Alarm being triggered; (**c**) The azimuth plot of T$_b$ fell in the region of 225° to 270°.

Considering the complexity of the urban setting, high-density urban development would hinder extensive tree root habitats. The overall process of tree anchorage resistance can be generally categorized into two phases [53]. The soil tensile strength dominates at the very beginning and shears to resist uprooting, while the resistance diminishes quickly when the mechanical stress reaches the leeward root hinge point. The stem base further pushes away the root-plate from vertical to the side of around 4°, as postulated by England [54]. Then, the root tensile strength, stem weight, and tree weight take up the dominant part to resist uprooting and overturning [55–57]. While tree anchorage is failed, the tree will collapse. Tree anchorage can be determined by Fourcaud et al. [55]:

$$
\begin{aligned}
\textit{Tree anchorage} \quad &= (\textit{Root volumn or mass}) \\
&\times (\textit{leeward hinge distance from stem base})
\end{aligned}
\tag{2}
$$

The analysis of tilt angles under wind regimes demonstrates the underlying risk factors of root displacement and provides important indicators for the advisability of tree felling [58]. Falling tree T_a underwent at least two storm events and experienced excessive tilt movements twice before tree failure. T_b's failure occurred in a single storm event that caused its drastic collapse. T_a was extraordinary in relation to tilt behavior over the two-month monitoring period. Tilt analysis of T_a stability indicated plausible root failure due to reduced soil–root anchoring ability. The presence of fungi decay and termite infestation is likely one of the causes attributed to tree-fall; leading to reduced tree vitality and lower soil suction [57]. As a result of the cavities at the lower base of T_a, it was speculated that the trunk of T_a was defective prior to exposure to high winds during storm occurrence, reducing the wind resistance force [59]. Other factors such as root size and distribution, soil characteristics, and history of wind gusts were also significant causative factors since all these parameters would have affected the tensile resistance to uprooting events [10,14,60]. The data showed that the tilt angle exceeded the threshold values, which triggered the Increasing Trend Alarm in the first wave of the rainstorm and the second wave of Typhoon Higos, meaning that immediate attention is needed.

On the other hand, T_b was planted near a concrete-paved sloping site where the growth and development of lateral roots were limited. In general, the tree stem was angularly displaced in an elliptic shape along the main wind direction and distributes transverse stress symmetrically onto the root system and tree trunk to withstand wind [14,57], through which the trees can survive by resisting overturning under high wind environments [61,62]. When the leeward root hinge breaks, the root no longer resists uprooting. The failure of T_b which triggered the Sudden Alarm was likely caused by an underdeveloped soil–root system generating sudden failure under wind load [63,64].

3.2. Wind Simulation of Fallen Trees in the Built Environment

Some trees are susceptible to wind [20]. Wind data can help simulate the intensity of wind flow under complex-built environments and permit the examination of interactions between wind dynamics and uprooting failure. In urban areas, wind tunnel effects where wind is funneled between tall buildings are very common [65]. Simulations of these effects can be undertaken by Airflow Computational Fluid Dynamics (CFD) to demonstrate wind flow in urban settings before and during a typhoon. The relevant parameters for tree tilt and sway behavior analysis of a sturdy tree, such as wind speed and direction, were collected from the designated weather station of Kai Tak (Figure 7).

The weather record shows that wind speeds intensified to 66 km/h during Higos, which was approximately four times that of normal days. On 18 August 2020, the wind force on tree T_a was 36.7 km/h, despite highly weakened by the built environment, which was presumably from a south-easterly direction during the Strong Wind Signal (Signal No. 3). The change of the prevailing wind direction may lead to tree T_a fell before the Increasing Gale or Storm Signal (Signal No. 9) on 19 August 2020.

On the contrary, the windthrown tree T_b fell under lower wind speeds between 5 and 8 km/h on 19 August 2020, when Increasing Gale or Storm Signal No. 9 was hoisted. Notwithstanding the low wind speed recorded on that morning, the impact of wind gusts cannot be underestimated. The Kai Tak weather station recorded wind gusts above 30 km/h, even reaching a maximum of 43 km/h between 10 a.m. and 11 a.m. on 19 August 2020 when the tree collapsed. Furthermore, on normal weather days, the simulation of wind speed at T_b is less than 2 km/h and this very low wind speed is likely caused by wind tunnel effects being filtered by nearby high-rise buildings. It is speculated that T_b is more wind prone and adapted to far smaller wind loading than T_a as its wind flow is usually below 1.5 km/h, compared to above 20 km/h at T_a. Coupled with the rainfall having lowered soil cohesion, the strength of soil–root anchorage of T_b was substantially reduced and more vulnerable to the wind.
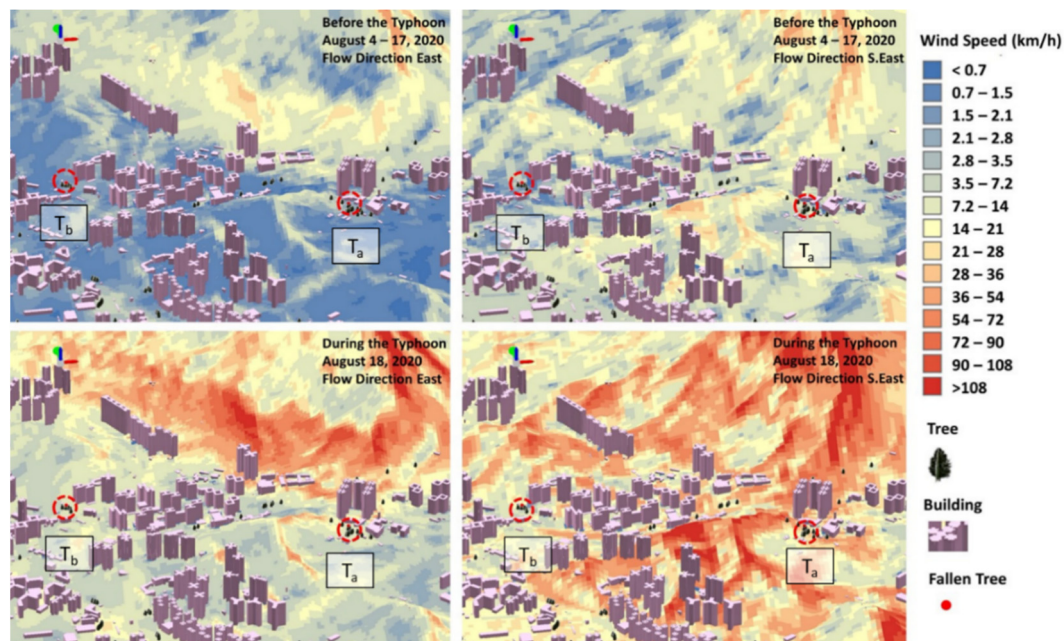
Figure 7. Computational Fluid Dynamics (CFD) model before and during the typhoon.

The findings of this study combine the collected tilt angle with wind speed and wind direction. The CFD model gives a more accurate simulation to understand the relationship between dynamic-wind flow and trees in the affected areas when very limited in-situ wind measurements are available. Therefore, extending the analyses with inflow wind data of each tree would provide a better understanding of the scientific evidence to tree management personnel for risk preparedness.

The two fallen trees both exhibited similar mechanical features of permanent displacement; their tilt movement was excessive before coming to a halt within a short time following the abnormality. The study permitted the development of Increasing Trend Alarm and Sudden Increase Alarm, based upon millions of data entries from thousands of sensors over the previous months. These alarms can statistically detect tree failure due to weakened root anchorage. Our data analysis identifies a two-fold tree failure pattern. First, the result from tree T_a shows that the Increasing Trend Alarm is triggered during the first and second waves of excessive tilt increase, alerting the tree manager to take necessary action from further leaning. Second, the Sudden Alarm of tree T_b is triggered during its collapse and provides an alert notification and information to the tree maintenance departments, which is valuable data in developing contingency plans to mitigate hazards during typhoons.

3.3. Analyses of Tree Tilt Pattern

3.3.1. Overall Change in Tilt Angle before and after Typhoon

Figure 8 shows the variation of tilt angle difference among all 18 species. The differences in tilt angle to wind response were generally below 0.5°, except for *Eucalyptus citrodora* trees which have a relatively higher median value. As most *Eucalyptus citrodora* trees were planted at amenity plots in urban areas, the unusual variation is likely due to the root underdevelopment of the species, as Eucalypt trees tend to have wide-ranging root formations [66].
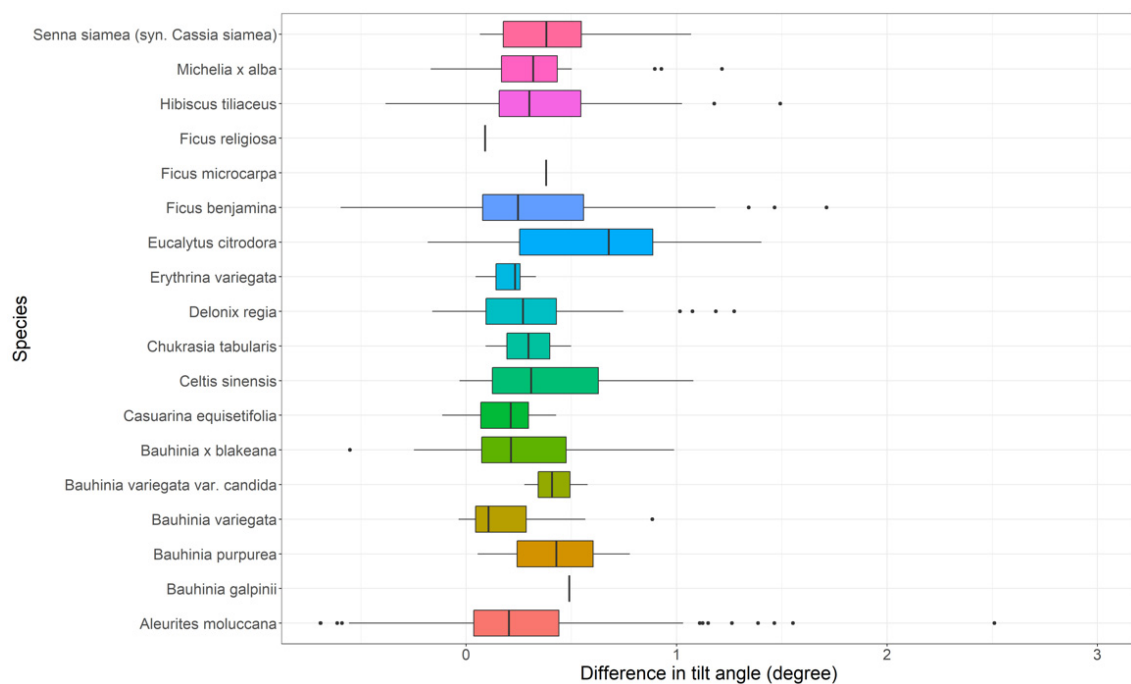
Figure 8. Boxplot for the change of tilt angles against tree species in pre- and post-typhoon among 856 trees without collapsed trees included.

Further statistical analysis was done to investigate the correlation between tree tilt angle and tree attributes. To ensure data integrity, targeted trees with incomplete tilt angle records during the typhoon period, or extreme tilt angle changes due to signal transmission problems, were excluded. Some sensor data were removed with the last data record being exceeded for more than 12 h after the typhoon warning signal was canceled, since these values were recorded after the typhoon period that could not statistically represent the condition of tree tilt. Additionally, the dataset of species with less than 20 individuals were also excluded for that subset. Among 889 individual sensor data, 856 sets of data fulfilled the criteria and were valid in the analysis, covering nine species, i.e., *Senna siamea* (syn. *Cassia siamea*), *Michelia x alba*, *Hibiscus tiliaceus*, *Ficus benjamina*, *Delonix regia*, *Celtis sinensis*, *Casuarina equisetifolia*, *Bauhinia x blakeana*, and *Aleurites moluccana*.

3.3.2. ANCOVA Results of between Attributes Effect to Tree Tilt Angle

Analysis of Covariance (ANCOVA) was conducted to investigate the interaction result of tree attributes to tilt angle. The covariates include DBH, tree height, crown spread, and species. Table 1 demonstrates that the interaction result of tilt angle from ANCOVA is significant to species with $F(8, 844) = 2.4693$ and $p = 0.0120$ ($\alpha < 0.05$), but DBH, crown spread, and height were not statistically different among tilt angle within any species. Therefore, tree species is the determinant of tree tilt when compared with other parameters. The result is similar to [67–69] showing that species are more dominant relative to the likelihood of failure during windstorms.

3.3.3. Tree Tilt Comparison between Species

From the result of Table 1, analysis was made by comparing the tree tilt with respect to species, and the descriptive statistics are listed in Table 2. The distribution of tree species *Aleurites moluccana* is 47.55%, which has the largest proportion in the subset, followed by *Ficus benjamina* with 23.19% and *Delonix regia* with 9.65%. *Aleurites moluccana* is a fast-growing and exotic species, and the government was in favor of planting this species on roadsides and parks in the past few decades to improve streetscapes [36].

Table 1. ANCOVA results of between attribute effects and tree tilt angle.

Dependent Variable	Tilt Angle Difference				
	Type III Sum of Squares	df	Mean Square	F	*p*-Value
Corrected Model	5.076 *	11	0.4615	2.1480	0.0154
Intercept	4.7418	1	4.7418	22.0709	0.0000
DBH	0.3961	1	0.3961	1.8438	0.1749
Crown Spread	0.2853	1	0.2853	1.3279	0.2495
Height	0.0023	1	0.0023	0.0109	0.9170
Species	4.2442	8	0.5305	2.4693	0.0120
Error	181.3295	844	0.2148		
Total	297.9397	856			
Corrected Total	186.4059	855			

* R Squared = 0.027 (Adjusted R Squared = 0.015).

Table 2. Descriptive statistics of tree tilt angle by species.

Species	N	Percentage	Mean	SD	SE	IQR	95% CI	
							Lower Bound	Upper Bound
Senna siamea (syn. Cassia siamea)	18	2.33%	0.4598	0.2642	0.0623	0.3183	0.3284	0.5912
Michelia x alba	21	2.44%	0.4423	0.3637	0.0794	0.3424	0.2768	0.6079
Hibiscus tiliaceus	38	4.42%	0.4810	0.4978	0.0807	0.3616	0.3174	0.6446
Ficus benjamina	199	23.14%	0.4496	0.6801	0.0482	0.5198	0.3545	0.5447
Delonix regia	83	9.65%	0.3770	0.3160	0.0347	0.3462	0.3080	0.4460
Celtis sinensis	31	3.72%	0.4261	0.3194	0.0574	0.5648	0.3090	0.5433
Casuarina equisetifolia	23	2.67%	0.2354	0.1517	0.0316	0.2841	0.1698	0.3010
Bauhinia x blakeana	36	4.19%	0.3076	0.3591	0.0599	0.4550	0.1861	0.4291
Aleurites moluccana	407	47.44%	0.3014	0.3878	0.0192	0.4442	0.2636	0.3392
Total	856							

N: Number of samples, SD: Standard deviation, SE: Standard error, IQR: Interquartile range, CI: Confidence interval.

One-way ANOVA was performed to evaluate the contribution of species to tilt angle. The result indicates statistical significance $p = 0.008$ ($\alpha < 0.05$) between species group and the dependent variable of tilt angle difference (Table 3).

Table 3. Results of one-way ANOVA by species.

Variation Sources	Sum of Squares	df	Mean Square	F	*p*-Value
Between species	4.4870	8	0.5609	2.6114	0.0080 *
Within species	181.9189	847	0.2148		
Total	186.4059	855			

* indicates significant result with *p*-Value < 0.05.

Tukey's post hoc tests for multiple comparison was applied to the hypothesis to investigate the relationship among each species over the typhoon period. Since the sample size is unequal, the harmonic mean of group size is applied. Table 4 shows the comparison of species with significant results only. The results indicate that the mean difference of tilt angle is significant between the tree species *Ficus benjamina* and *Aleurites moluccana*, i.e., $p = 0.0072$ ($\alpha < 0.05$) but not significant in other species. Both species have shown similar growth conditions, many of which were pavement and roadside trees.

Table 4. Tukey's post hoc tests for multiple comparisons (species with significant results only).

Species 1	Species 2	MD	SE	*p*-Value	95% CI	
					Lower Bound	**Upper Bound**
Ficus benjamina	*Senna siamea (syn. Cassia siamea)*	−0.0102	0.1141	1.0000	−0.3649	0.3445
	Michelia x alba	0.0073	0.1063	1.0000	−0.3234	0.3380
	Hibiscus tiliaceus	−0.0314	0.0820	1.0000	−0.2866	0.2237
	Delonix regia	0.0726	0.0606	0.9569	−0.1158	0.2609
	Celtis sinensis	0.0235	0.0895	1.0000	−0.2548	0.3018
	Casuarina equisetifolia	0.2142	0.1021	0.4749	−0.1032	0.5316
	Bauhinia x blakeana	0.1420	0.0839	0.7518	−0.1190	0.4030
	Aleurites moluccana	**0.1481 ***	**0.0401**	**0.0072**	**0.0235**	**0.2728**
Aleurites moluccana	*Senna siamea (syn. Cassia siamea)*	−0.1584	0.1116	0.8906	−0.5055	0.1887
	Michelia x alba	−0.1409	0.1037	0.9128	−0.4634	0.1816
	Hibiscus tiliaceus	−0.1796	0.0786	0.3525	−0.4241	0.0649
	Ficus benjamina	**−0.1481 ***	**0.0401**	**0.0072**	**−0.2728**	**−0.0235**
	Delonix regia	−0.0756	0.0558	0.9141	−0.2492	0.0980
	Celtis sinensis	−0.1247	0.0863	0.8803	−0.3932	0.1438
	Casuarina equisetifolia	0.0660	0.0993	0.9992	−0.2429	0.3749
	Bauhinia x blakeana	−0.0062	0.0806	1.0000	−0.2568	0.2444

* indicates significant result with p-Value < 0.05, MD: Mean difference, SE: Standard error, CI: Confidence interval.

Within the study, the native species, *Ficus benjamina* trees in Hong Kong, were frequently attacked by a fungal disease that usually developed decay on the buttress root or trunk base, weakening the anchor support for the entire tree. *Ficus* species are included as one of the most common failure trees during typhoons with a weak anchor to the soil [70].

Aleurites moluccana trees have higher potential for being associated with limited growth habitat, tall tree structure, and narrow crown spread, as stated by [71–73], and this tree species is more prone to uprooting failure. Yet the tilt response of this species performed more stably under typhoon Higos as compared to other species. It might likely have proper pruning and maintenance before the typhoon as this species is frequently planted on the roadside and parks in Hong Kong.

Overall, there may be differentiation from some studies speculating the relationships between wind and tree sway [14,58,63,74], and stated that tree size can directly correlate with and influence tree motion [35,75,76]. Presumably, this aspect shows a limitation in our approach where tilt responses can vary from different trees in an urban setting. Exploring and quantifying the tilt response of each tree requires dedicated studies with a focus on their tree dimensions and surrounding features. Therefore, there needs to be enough data to capture the relationships that may exist between the parameters and the tilt angles from continuous monitoring.

4. Conclusions

The urban environment is spatially heterogeneous and varies temporally; therefore, the cause of tree failure is complex. This paper presents tilt data of 889 trees pre-and during the typhoon, of which two urban trees collapsed during Typhoon Higos in 2020 serve as a case study to demonstrate tree response to windstorm.

The tilt variations of two fallen trees—both exhibited similar mechanical features of permanent displacement; their tilt movement was excessive before coming to a halt within a short time following the abnormality. The study permits the development of the Increasing Trend Alarm and Sudden Increase Alarm, based upon millions of data entries from thousands of sensors over the previous months. These alarms can statistically detect tree failure due to weakened root anchorage. Furthermore, the results indicated that changes in tilt angles under Typhoon Higos are varied by species, mainly due to the gusty wind, though further validation with a larger sample size is essential. The limitation

may apply to this study; unexpected site variables, such as ground vibration from the construction work nearby, may interfere with tilt variations, adding complexity to set up control samples in the urban districts. Ideally, control experiments should be established in a closed environment, but this could not be carried out under the scope of this study.

In conclusion, this preliminary investigation could serve as a foundation of research on the relationship between tilt angle change and quantifiable structural parameters. Based on the current dataset, the establishment of the dynamic baseline of threshold values tests works, and this allows an initial starting point to compare the tilt response of individual trees and among the species in urban forests [47]. It is highly recommended that future research of this type collects additional data to further develop a tree risk index where a holistic tilt monitoring system is vital for urban tree management that can go beyond simply identifying which trees require a safety inspection [39]. It could embed algorithms with a frontend dashboard to show the real-time data that would add benefits by providing a more precise early-stage detection to recognize unanticipated potential tree failure, while the development of comprehensive risk control can help facilitate tree management in cities and protect human life during future climate regimes.

5. Patents

A short-term patent has been granted for the invention "Tree Monitoring System for Urban Tree Management" with reference no.: JHC/U20154HK00.

References

1. Bolund, P.; Hunhammar, S. Ecosystem Services in Urban Areas. *Ecol. Econ.* **1999**, *29*, 293–301. [CrossRef]
2. Gómez-Baggethun, E.; Barton, D.N. Classifying and Valuing Ecosystem Services for Urban Planning. *Ecol. Econ.* **2013**, *86*, 235–245. [CrossRef]
3. Salbitano, F.; Borelli, S.; Conigliaro, M.; Chen, Y. *Guidelines on Urban and Peri-Urban Forestry. FAO Forestry Paper No. 178*; Food and Agriculture Organization of the United Nations: Rome, Italy, 2016.
4. Tyrväinen, L.; Pauleit, S.; Seeland, K.; de Vries, S. Benefits and Uses of Urban Forests and Trees. In *Urban Forests and Trees*; Konijnendijk, C., Nilsson, K., Randrup, T., Schipperijn, J., Eds.; Springer: Berlin/Heidelberg, Germany, 2005; pp. 81–114.
5. Dunster, J.A.; Smiley, E.T.; Matheny, N.; Lilly, S. *Tree Risk Assessment Manual*, 2nd ed.; International Society of Arboriculture: Champaign, IL, USA, 2017.
6. Ellison, M.J. Quantified Tree Risk Assessment Used in the Management of Amenity Trees. *J. Arboric.* **2005**, *31*, 57–65. [CrossRef]
7. Koeser, A.K.; Thomas Smiley, E.; Hauer, R.J.; Kane, B.; Klein, R.W.; Landry, S.M.; Sherwood, M. Can Professionals Gauge Likelihood of Failure?—Insights from Tropical Storm Matthew. *Urban For. Urban Green.* **2020**, *52*, 126701. [CrossRef]
8. Marszal, E.M. Tolerable Risk Guidelines. *ISA Trans.* **2001**, *40*, 391–399. [CrossRef]

9. Moore, J.R. Differences in Maximum Resistive Bending Moments of Pinus Radiata Trees Grown on a Range of Soil Types. *For. Ecol. Manag.* **2000**, *135*, 63–71. [CrossRef]

10. Dupuy, L.; Fourcaud, T.; Stokes, A. A Numerical Investigation into Factors Affecting the Anchorage of Roots in Tension. *Eur. J. Soil Sci.* **2005**, *56*, 319–327. [CrossRef]

11. Kim, Y.; Rahardjo, H.; Tsen-Tieng, D.L. Stability Analysis of Laterally Loaded Trees Based on Tree-Root-Soil Interaction. *Urban For. Urban Green.* **2020**, *49*, 126639. [CrossRef]

12. Detter, A.; van Wassenaer, P.; Rust, S. Stability Recovery in London Plane Trees Eight Years After Primary Anchorage Failure. *Arboric. Urban For.* **2019**, *45*, 279–288. [CrossRef]

13. Boose, E.R.; Foster, D.R.; Fluet, M. Hurricane Impacts to Tropical and Temperate Forest Landscapes. *Ecol. Monogr.* **1994**, *64*, 369–400. [CrossRef]

14. Yang, M.; Défossez, P.; Dupont, S. A Root-to-Foliage Tree Dynamic Model for Gusty Winds during Windstorm Conditions. *Agric. For. Meteorol.* **2020**, *287*, 107949. [CrossRef]

15. Zimmerman, J.K.; Everham III, E.M.; Waide, R.B.; Lodge, D.J.; Taylor, C.M.; Brokaw, N.V.L. Responses of Tree Species to Hurricane Winds in Subtropical Wet Forest in Puerto Rico: Implications for Tropical Tree Life Histories. *J. Ecol.* **1994**, *82*, 911. [CrossRef]

16. Government of HKSAR. LCQ8: Tree Management. Available online: https://www.info.gov.hk/gia/general/201801/17/P20180 11700827.htm (accessed on 5 November 2021).

17. Hong Kong Observatory. Typhoon Higos (2007) 17 to 19 August 2020. Available online: https://www.hko.gov.hk/en/informtc/ higos20/report.html (accessed on 5 November 2021).

18. Pachauri, R.K.; Allen, M.R.; Barros, V.R.; Broome, J.; Cramer, W.; Christ, R.; Church, J.A.; Clarke, L.; Dahe, Q.; Dasgupta, P.; et al. *Climate Change 2014: Synthesis Report. Contribution of Working Groups I, II and III to the Fifth Assessment Report of the Intergovernmental Panel on Climate Change*; Pachauri, R., Meyer, L., Eds.; IPCC: Geneva, Switzerland, 2014; ISBN 9789291691432.

19. van Wassenaer, P.; Richardson, M. A Review of Tree Risk Assessment Using Minimally Invasive Technologies and Two Case Studies. *Arboric. J.* **2009**, *32*, 275–292. [CrossRef]

20. Jackson, T.; Shenkin, A.; Moore, J.; Bunce, A.; van Emmerik, T.; Kane, B.; Burcham, D.; James, K.; Selker, J.; Calders, K.; et al. An Architectural Understanding of Natural Sway Frequencies in Trees. *J. R. Soc. Interface* **2019**, *16*, 20190116. [CrossRef]

21. Ball, D.J.; Watt, J. Further Thoughts on the Utility of Risk Matrices. *Risk Anal.* **2013**, *33*, 2068–2078. [CrossRef] [PubMed]

22. Cox, L.A., Jr. What's Wrong with Risk Matrices? *Risk Anal.* **2008**, *28*, 497–512. [CrossRef] [PubMed]

23. Cox, L.A.; Babayev, D.; Huber, W. Some Limitations of Qualitative Risk Rating Systems. *Risk Anal.* **2005**, *25*, 651–662. [CrossRef] [PubMed]

24. O'sullivan, M.F.; Ritchie, R.M. Tree Stability in Relation to Cyclic Loading. *Forestry* **1993**, *66*, 69–82. [CrossRef]

25. Webb, E.L.; van de Bult, M.; Fa'aumu, S.; Webb, R.C.; Tualaulelei, A.; Carrasco, L.R. Factors Affecting Tropical Tree Damage and Survival after Catastrophic Wind Disturbance. *Biotropica* **2014**, *46*, 32–41. [CrossRef]

26. Jahani, A.; Saffariha, M. Modeling of Trees Failure under Windstorm in Harvested Hyrcanian Forests Using Machine Learning Techniques. *Sci. Rep.* **2021**, *11*, 1124. [CrossRef]

27. Krišāns, O.; Matisons, R.; Kitenberga, M.; Donis, J.; Rust, S.; Elferts, D.; Jansons, Ā. Wind Resistance of Eastern Baltic Silver Birch (Betula Pendula Roth.) Suggests Its Suitability for Periodically Waterlogged Sites. *Forests* **2020**, *12*, 21. [CrossRef]

28. Liu, M.; Zhang, D.; Pietzarka, U.; Roloff, A. Assessing the Adaptability of Urban Tree Species to Climate Change Impacts: A Case Study in Shanghai. *Urban For. Urban Green.* **2021**, *62*, 127186. [CrossRef]

29. Ilyas, M.; Liu, Y.-Y.; Shah, S.; Ali, A.; Khan, A.H.; Zaman, F.; Yucui, Z.; Saud, S.; Adnan, M.; Ahmed, N.; et al. Adaptation of Functional Traits and Their Plasticity of Three Ornamental Trees Growing in Urban Environment. *Sci. Hortic.* **2021**, *286*, 110248. [CrossRef]

30. Jim, C.Y. Improving Soil Specification for Landscape Tree Planting in the Tropics. *Landsc. Urban Plan.* **2021**, *208*, 104033. [CrossRef]

31. Koeser, A.K.; Klein, R.W.; Hasing, G.; Northrop, R.J. Factors Driving Professional and Public Urban Tree Risk Perception. *Urban For. Urban Green.* **2015**, *14*, 968–974. [CrossRef]

32. Serafin, A.; Wynalda, B. Trees Take the Streets: Urban Tree Growth and Hazard Potential. *SUURJ Seattle Univ. Undergrad. Res. J.* **2021**, *5*, 12.

33. Lonsdale, D. *Principles of Tree Hazard Assessment and Management*; Stationery Office Ltd, Publications Centre: London, UK, 1999.

34. Kim, Y.; Rahardjo, H.; Tsen-Tieng, D.L. Mechanical Behavior of Trees with Structural Defects under Lateral Load: A Numerical Modeling Approach. *Urban For. Urban Green.* **2021**, *59*, 126987. [CrossRef]

35. Jackson, T.D.; Sethi, S.; Dellwik, E.; Angelou, N.; Bunce, A.; van Emmerik, T.; Duperat, M.; Ruel, J.-C.; Wellpott, A.; van Bloem, S.; et al. The Motion of Trees in the Wind: A Data Synthesis. *Biogeosciences* **2021**, *18*, 4059–4072. [CrossRef]

36. Jim, C.Y. Tree-Habitat Relationships in Urban Hong Kong. *Biol. Conserv.* **1993**, *66*, 150. [CrossRef]

37. Vojáčková, B.; Tippner, J.; Horáček, P.; Sebera, V.; Praus, L.; Mařík, R.; Brabec, M. The Effect of Stem and Root-Plate Defects on the Tree Response during Static Loading—Numerical Analysis. *Urban For. Urban Green.* **2021**, *59*, 127002. [CrossRef]

38. Lee, L.S.H.; Jim, C.Y. Applying Precision Triaxial Accelerometer to Monitor Branch Sway of an Urban Tree in a Tropical Cyclone. *Landsc. Urban Plan.* **2018**, *178*, 170–182. [CrossRef]

39. Göcke, L.; Rust, S.; Ruhl, F. Assessing the Anchorage and Critical Wind Speed of Urban Trees Using Root-Plate Inclination in High Winds. *Arboric. Urban For.* **2018**, *44*. [CrossRef]

40. Ossenbruggen, P.J.; Peters, M.A.; Shigo, A.L. Potential Failure of a Decayed Tree Under Wind Loading. *Wood Fiber Sci.* **1986**, *18*, 168–186.
41. Rust, S. Tree Inventory, Risk Assessment and Management. In *Urban Tree Management: For the Sustainable Development of Green Cities*; Roloff, A., Ed.; John Wiley and Sons: Hoboken, NJ, USA, 2015; p. 111.
42. Duryea, M.L.; Kampf, E. *Wind and Trees: Lessons Learned from Hurricanes*; EDIS: Gainesville, FL, USA, 2007.
43. Duryea, M.L.; Kampf, E.; Littell, R.C.; Rodriguez-Pedraza, C.D. Hurricanes and the Urban Forest: II. Effects on Tropical and Subtropical Tree Species. *Arboric. Urban For.* **2007**, *33*, 98–112. [CrossRef]
44. James, K.; Hallam, C.; Spencer, C. Tree Stability in Winds: Measurements of Root Plate Tilt. *Biosyst. Eng.* **2013**, *115*, 324–331. [CrossRef]
45. James, K.; Hallam, C.; Spencer, C. Measuring Tilt of Tree Structural Root Zones under Static and Wind Loading. *Agric. For. Meteorol.* **2013**, *168*, 160–167. [CrossRef]
46. Sellier, D.; Fourcaud, T. Crown Structure and Wood Properties: Influence on Tree Sway and Response to High Winds. *Am. J. Bot.* **2009**, *96*, 885–896. [CrossRef]
47. Abbas, S.; Kwok, C.Y.T.; Hui, K.K.W.; Li, H.; Chin, D.C.W.; Ju, S.; Heo, J.; Wong, M.S. Tree Tilt Monitoring in Rural and Urban Landscapes of Hong Kong Using Smart Sensing Technology. *Trees For. People* **2020**, *2*, 100030. [CrossRef]
48. Hong Kong Observatory. The Year's Weather. 2020. Available online: https://www.hko.gov.hk/en/wxinfo/pastwx/2020/ywx2020.htm (accessed on 5 November 2021).
49. Hong Kong Observatory. Tropical Cyclone Annual Publications. Available online: https://www.hko.gov.hk/en/publica/pubtc.htm (accessed on 5 November 2021).
50. Terho, M. An Assessment of Decay among Urban Tilia, Betula, and Acer Trees Felled as Hazardous. *Urban For. Urban Green.* **2009**, *8*, 77–85. [CrossRef]
51. Selbig, W.R.; Loheide, S.P.; Shuster, W.; Scharenbroch, B.C.; Coville, R.C.; Kruegler, J.; Avery, W.; Haefner, R.; Nowak, D. Quantifying the Stormwater Runoff Volume Reduction Benefits of Urban Street Tree Canopy. *Sci. Total Environ.* **2022**, *806*, 151296. [CrossRef]
52. Hothorn, T.; Bretz, F.; Westfall, P. Simultaneous Inference in General Parametric Models. *Biom. J.* **2008**, *50*, 346–363. [CrossRef] [PubMed]
53. Peltola, H.M. Mechanical Stability of Trees under Static Loads. *Am. J. Bot.* **2006**, *93*, 1501–1511. [CrossRef] [PubMed]
54. England, A.H. A Dynamic Analysis of Windthrow of Trees. *Forestry* **2000**, *73*, 225–238. [CrossRef]
55. Fourcaud, T.; Ji, J.-N.; Zhang, Z.-Q.; Stokes, A. Understanding the Impact of Root Morphology on Overturning Mechanisms: A Modelling Approach. *Ann. Bot.* **2007**, *101*, 1267–1280. [CrossRef]
56. van Haaften, M.; Liu, Y.; Wang, Y.; Zhang, Y.; Gardebroek, C.; Heijman, W.; Meuwissen, M. Understanding Tree Failure—A Systematic Review and Meta-Analysis. *PLoS ONE* **2021**, *16*, e0246805. [CrossRef]
57. Mattheck, C.; Breloer, H. *The Body Language of Trees: A Handbook for Failure Analysis*; HMSO Publications Centre: London, UK, 1994.
58. Moore, J.; Gardiner, B.; Sellier, D. Tree Mechanics and Wind Loading. In *Plant Biomechanics*; Geitmann, A., Gril, J., Eds.; Springer International Publishing: Cham, Switzerland, 2018; pp. 79–106.
59. Clair, B.; Fournier, M.; Prevost, M.F.; Beauchene, J.; Bardet, S. Biomechanics of Buttressed Trees: Bending Strains and Stresses. *Am. J. Bot.* **2003**, *90*, 1349–1356. [CrossRef]
60. Zhou, W.-H.; He, S.-Y.; Garg, A.; Yin, Z.-Y. Field Monitoring of Suction in the Vicinity of an Urban Tree: Exploring Termite Infestation and the Shading Effects of Tree Canopy. *Acta Geotech.* **2020**, *15*, 1341–1361. [CrossRef]
61. Pivato, D.; Dupont, S.; Brunet, Y. A Simple Tree Swaying Model for Forest Motion in Windstorm Conditions. *Trees* **2014**, *28*, 281–293. [CrossRef]
62. Schaetzl, R.J.; Johnson, D.L.; Burns, S.F.; Small, T.W. Tree Uprooting: Review of Terminology, Process, and Environmental Implications. *Can. J. For. Res.* **1989**, *19*, 1–11. [CrossRef]
63. Moore, G.M. Wind-Thrown Trees: Storms or Management? *Arboric. Urban For.* **2014**, *40*, 53–69. [CrossRef]
64. Yang, Z.; Hui, K.W.; Abbas, S.; Zhu, R.; Kwok, C.Y.T.; Heo, J.; Ju, S.; Wong, M.S. A Review of Dynamic Tree Behaviors: Measurement Methods on Tree Sway, Tree Tilt, and Root–Plate Movement. *Forests* **2021**, *12*, 379. [CrossRef]
65. Kalmikov, A.; Dupont, G.; Dykes, K.; Chan, C.P. Wind Power Resource Assessment in Complex Urban Environments: MIT Campus Case-Study Using CFD Analysis. In Proceedings of the AWEA 2010 WINDPOWER Conference, Dallas, TX, USA, 23–26 May 2010.
66. Sigunga, D.O.; Kimura, M.; Hoshino, M.; Asanuma, S.; Onyango, J.C. Root-Fusion Characteristic of Eucalyptus Trees Block Gully Development. *J. Environ. Prot.* **2013**, *4*, 877–880. [CrossRef]
67. Foster, D.R. Disturbance History, Community Organization and Vegetation Dynamics of the Old-Growth Pisgah Forest, South-Western New Hampshire, U.S.A. *J. Ecol.* **1988**, *76*, 105. [CrossRef]
68. Gibbs, J.N.; Greig, B.J.W. Survey of Parkland Trees after the Great Storm of October 16, 1987. *Arboric. J.* **1990**, *14*, 321–347. [CrossRef]
69. Putz, F.E.; Sharitz, R.R. Hurricane Damage to Old-Growth Forest in Congaree Swamp National Monument, South Carolina, U.S.A. *Can. J. For. Res.* **1991**, *21*, 1765–1770. [CrossRef]

70. Lin, H.; Huang, S.; Gu, Y.; Chen, Z.; Lu, Y.; Yin, S.; Jin, H.; Wu, W.; Xiao, Y. Risk Assessments of Trees and Urban Spaces under Attacks of Typhoons: A Survey and Statistical Study in Guangzhou, China. *IOP Conf. Ser. Earth Environ. Sci.* **2020**, *588*, 032055. [CrossRef]

71. Jim, C.Y. Roadside Trees in Urban Hong Kong: Part IV Tree Growth and Environmental Condition. *Arboric. J.* **1997**, *21*, 89–106. [CrossRef]

72. Jim, C.Y.; Liu, H.H.T. Storm Damage on Urban Trees in Guangzhou, China. *Landsc. Urban Plan.* **1997**, *38*, 45–59. [CrossRef]

73. Chau, N.L.; Jim, C.Y.; Zhang, H. Species-Specific Holistic Assessment of Tree Structure and Defects in Urban Hong Kong. *Urban For. Urban Green.* **2020**, *55*, 126813. [CrossRef]

74. Rutledge, B.T.; Cannon, J.B.; McIntyre, R.K.; Holland, A.M.; Jack, S.B. Tree, Stand, and Landscape Factors Contributing to Hurricane Damage in a Coastal Plain Forest: Post-Hurricane Assessment in a Longleaf Pine Landscape. *For. Ecol. Manag.* **2021**, *481*, 118724. [CrossRef]

75. Stubbs, C.J.; Cook, D.D.; Niklas, K.J. A General Review of the Biomechanics of Root Anchorage. *J. Exp. Bot.* **2019**, *70*, 3439–3451. [CrossRef] [PubMed]

76. Wonn, H.T.; O'Hara, K.L. Height: Diameter Ratios and Stability Relationships for Four Northern Rocky Mountain Tree Species. *West. J. Appl. For.* **2001**, *16*, 87–94. [CrossRef]